# *Fast switching and signature of efficient domain wall motion driven by spin-orbit torques in a perpendicular anisotropy magnetic insulator/Pt bilayer*

# Fast switching and signature of efficient domain wall motion driven by spin-orbit torques in a perpendicular anisotropy magnetic insulator/Pt bilayer

Can Onur Avci, , Ethan Rosenberg, , Manuel Baumgartner, , Lukáš Beran, , Andy Quindeau, , Pietro Gambardella, , Caroline A. Ross, and , and Geoffrey S. D. Beach

Citation: Appl. Phys. Lett. **111**, 072406 (2017); doi: 10.1063/1.4994050
View online: http://dx.doi.org/10.1063/1.4994050
View Table of Contents: http://aip.scitation.org/toc/apl/111/7
Published by the American Institute of Physics

# Fast switching and signature of efficient domain wall motion driven by spin-orbit torques in a perpendicular anisotropy magnetic insulator/Pt bilayer

Can Onur Avci,[1,a)] Ethan Rosenberg,[1] Manuel Baumgartner,[2] Lukáš Beran,[1,3] Andy Quindeau,[1,4] Pietro Gambardella,[2] Caroline A. Ross,[1] and Geoffrey S. D. Beach[1]
[1]*Department of Materials Science and Engineering, Massachusetts Institute of Technology, Cambridge, Massachusetts 02139, USA*
[2]*Department of Materials, ETH Zürich, CH-8093 Zürich, Switzerland*
[3]*Charles University, Ke Karlovu 3, 12116 Prague 2, Czech Republic*
[4]*Geballe Laboratory for Advanced Materials, Stanford University, Stanford, California 94305, USA*

(Received 3 July 2017; accepted 7 August 2017; published online 17 August 2017)

We report fast and efficient current-induced switching of a perpendicular anisotropy magnetic insulator thulium iron garnet by using spin-orbit torques (SOT) from the Pt overlayer. We first show that, with quasi-DC (10 ms) current pulses, SOT-induced switching can be achieved with an external field as low as 2 Oe, making TmIG an outstanding candidate to realize efficient switching in heterostructures that produce moderate stray fields without requiring an external field. We then demonstrate deterministic switching with fast current pulses ($\leq$20 ns) with an amplitude of $\sim 10^{12}$ A/m$^2$, similar to all-metallic structures. We reveal that, in the presence of an initially nucleated domain, the critical switching current is reduced by up to a factor of five with respect to the fully saturated initial state, implying efficient current-driven domain wall motion in this system. Based on measurements with 2 ns-long pulses, we estimate the domain wall velocity of the order of $\sim$400 m/s per j = $10^{12}$ A/m$^2$. *Published by AIP Publishing.* [http://dx.doi.org/10.1063/1.4994050]

All-electrical control of magnetization is key for the development of future spin-based electronic devices.[1] Conventionally, in spin valve and magnetic tunnel junction devices, a charge current flowing between two ferromagnets is used to carry spin angular momentum and provide electrical switching, a phenomenon widely known as spin-transfer torque (STT).[2–6] However, more recently, spin-orbit torques (SOT) driven by the spin Hall (SHE) and interfacial effects have emerged as a more efficient alternative to the conventional STT approach.[7,8] In SOT, a pure spin current is generated transverse to a charge current flowing through a material with large spin-orbit coupling such as Pt or W, which can exert a magnetic torque on an adjacent ferromagnet. SOT consist of a damping-like (DL) torque with symmetry $\mathbf{T_{DL}} \propto \mathbf{m} \times (\mathbf{m} \times \mathbf{y})$ and a field-like (FL) torque with symmetry $\mathbf{T_{FL}} \propto \mathbf{m} \times \mathbf{y}$, where y is the in-plane (IP) axis perpendicular to the current injection direction.[9] SOT have been widely utilized to perform magnetization switching[8,10–17] and current-induced domain wall motion[18–22] in a variety of ferromagnetic/normal metal (NM) structures. To achieve SOT-induced switching, an in-plane field applied along the current direction is generally required to break the rotational symmetry of the magnetization.

Thus far, the majority of the SOT-related studies has been carried out on all-metallic ferromagnetic heterostructures. This is in part because they are easily accessible by electrical measurements (e.g., by Hall effect and magnetoresistance) but also because perpendicular magnetic anisotropy (PMA) can be easily obtained in these systems. However, magnetic insulators (MIs), such as iron-based garnets, possess remarkable properties such as ultralow damping and long magnon decay lengths, which can provide significant advantages for practical applications with respect to their metallic magnetic counterparts.[23–25] Therefore, exploiting SOT physics for device applications based on MIs is highly attractive from both fundamental and applied perspectives. Recently, SOT-driven magnetization switching of a MI thulium iron garnet/platinum (TmIG/Pt) bilayer possessing PMA has been demonstrated.[26] This achievement is potentially very useful for the development of memory and signal processing devices based on MIs, provided that the SOT-induced magnetization control can be achieved in ultra-short time scales and in devices with reduced lateral dimensions.

In this letter, we report on magnetization switching of TmIG/Pt bilayers with PMA with quasi-DC and sub-20 ns current pulses in micrometer-sized Hall cross structures. We first demonstrate that with 10 ms-long (quasi-DC) pulses, switching can be achieved with current density $j < 1 \times 10^{11}$ A/m$^2$ for an external in-plane field >35 Oe. By increasing the current density to $j = 2 \times 10^{11}$ A/m$^2$, the external field required for switching reduces to as low as 2 Oe, an exceptionally low value with respect to the literature. We then realize switching with 20 ns pulses with current density $j \sim 1 \times 10^{12}$ A/m$^2$. We reveal that the threshold switching current strongly depends on the absence or presence of an initially reversed domain in the structure. This implies that a relatively large current is required to nucleate a reversed domain starting from a fully saturated TmIG film, whereas very efficient domain wall propagation takes place in the non-saturated state. We estimate a domain wall velocity in TmIG of $\sim$400 m/s per $j = 1 \times 10^{12}$ A/m$^2$ based on measurements with 2 ns pulses and accounting for the geometrical characteristics, exceeding the most efficient domain wall velocities reported in metallic ferromagnets.

The TmIG ($Tm_3Fe_5O_{12}$, 9.6 nm) layer was grown by pulsed laser deposition on a (111) GGG ($Gd_3Ga_5O_{12}$) substrate at 900 °C in 150 mTorr of $O_2$ with a laser repetition

a)canavci@mit.edu

rate of 10 Hz and a substrate-target distance of 8 cm. Epitaxial growth of the TmIG films was confirmed via a high resolution x-ray diffraction $2\theta$-$\omega$ scan of the (444) reflection, and the film thickness was measured using x-ray reflectivity. The PMA originates primarily from magnetoelastic anisotropy in the strained film.[25,27] The saturation magnetization is 100 emu/cm$^{-3}$ based on vibrating sample magnetometry. Atomic force microscopy measurements indicated a root-mean-square roughness of 0.65 nm taken over a 1 $\mu$m$^2$ area. On top of TmIG, we grew Pt (4 nm) by magnetron sputtering. The continuous layer was patterned into symmetric Hall cross structures with nominal dimensions of $3 \times 3$ $\mu$m$^2$ by using standard optical lithography followed by $Ar^+$ ion milling.

Figure 1(a) shows a scanning electron micrograph of a typical device and the schematic of the measurement setup. For the Hall effect characterization and ms pulse experiments, we used the harmonic Hall voltage method to monitor the magnetization direction with an applied ac current and dc pulses of 10 ms for SOT-induced switching.[26,28] For the fast pulse experiments, we used a setup similar to the one described in Ref. 14. To ensure the transmission of fast current pulses without significant reflection, a 50 Ω resistance is connected in parallel with the device and 100 kΩ resistances are connected in series to prevent the spreading of high amplitude pulses into the Hall arms, as presented in Fig. 1(a). A magnetic field ($H_x$) is applied in-plane ($\theta_H = 90°$) along the x direction, parallel to the current. By using a bias tee, we separate the fast current pulses and the ac current used to probe the perpendicular component of the magnetization (not shown). All measurements were performed at room temperature.

In MI/normal metal (NM) bilayers, upon injecting a charge current, the SHE-driven spin current in the NM can

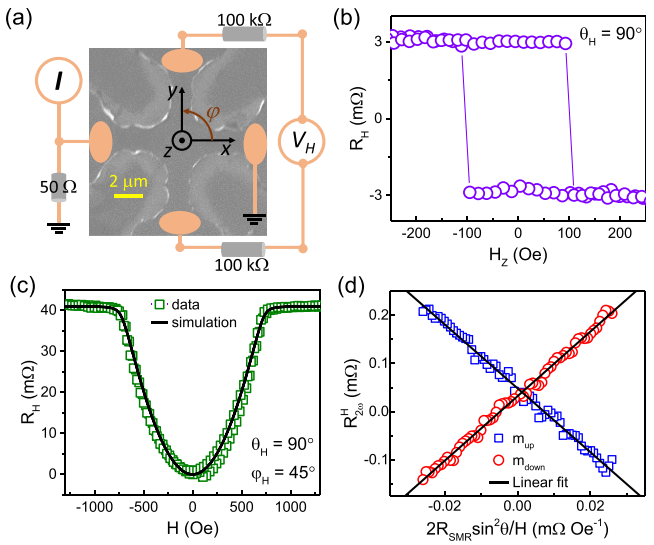


FIG. 1. (a) Scanning electron micrograph of a representative Hall cross device, electrical circuitry used for the fast pulse switching experiments, and the coordinate system. (b) Hall resistance measured during a field swept along the z direction. Hysteretic behavior of the curve with a coercivity of ~100 Oe reflects the large PMA of the TmIG/Pt bilayer system. (c) Hall resistance measured during an in-plane field sweep along $\varphi = 45°$. The characteristic U-shape behavior is due to coherent rotation of m towards in-plane [see Eq. (1)]. The black curve is a simulation based on a macrospin model and the experimental parameters. (d) Second harmonic Hall resistance measured for $\mathbf{m_{up}}$ and $\mathbf{m_{down}}$ with a field sweep along the y-axis, plotted versus the relevant quantity [see Eq. (2)] to extract the current-induced damping-like torque.

be absorbed or reflected at the interface depending on the magnetization direction of the MI. The back reflected spin current is converted into a charge current via the inverse SHE leading to a resistance change in the NM depending on the magnetization (**m**) orientation of MI.[29] This so-called spin Hall magnetoresistance (SMR) has also a transverse component that depends on the IP and out-of-plane (OOP) projections of **m** of the MI.[30] By considering the ordinary Hall effect of the NM, the resulting Hall resistance ($R_H$) is expressed as follows:[26]

$$R_H = R_{SMR}\sin^2\theta\sin 2\varphi + R_{AHE}\cos\theta + R_{OHE}H_z. \quad (1)$$

Here, $R_{SMR}$, $R_{AHE}$, and $R_{OHE}$ represent the transverse SMR, the SMR-induced anomalous Hall effect (AHE) resistance (with a possible contribution of AHE driven by the proximity induced polarization of Pt), and the ordinary Hall effect resistance of the NM, respectively. $\varphi$ and $\theta$ are the azimuthal and polar magnetization angles measured with respect to the x and z axes, respectively [see Fig. 1(a)]. We measure $R_H$ via a harmonic method where $R^H_\omega \equiv R_H$.

Figures 1(b) and 1(c) show $R^H_\omega$ as a function of OOP and IP field sweep, respectively. In the OOP field sweep, $R^H_\omega$ shows a clear hysteresis with ~100% remanence and a coercivity of ~100 Oe, characteristic of PMA. The IP field is applied at $\varphi = 45°$ where $R_{SMR}$ goes from zero when $\mathbf{m} \parallel \mathbf{z}$ to its maximum value when **m** is fully saturated in-plane ($\varphi = 45°$, $\theta = 90°$), see Eq. (1). The U-shape is characteristic for this type of measurement and is due to coherent rotation of **m** towards the plane.[25,26,31,32] The black curve is a simulation based on the macrospin approximation which fits accurately to the experimental data. From the data and simulation, we estimate the effective perpendicular anisotropy field of TmIG to be $H_K \approx 700$ Oe. From these two measurements, we obtain $R_{AHE} = 3$ mΩ and $R_{SMR} = 41$ mΩ. By considering the square resistance of $R_{sq} = 80$ Ω, we find $\frac{\Delta R_{SMR}}{R_{sq}} = 0.5 \times 10^{-3}$ similar to the largest reported values for Pt/MI[33–35] and ~5 times larger than the previous measurements on TmIG/Pt,[25,26,31] indicating a more efficient spin current generation and higher spin-mixing conductance of this particular TmIG/Pt interface. Following the expression given in Ref. 30 and using the experimental parameters determined above and literature values of the spin Hall angle $\theta_{SH} = 0.07$ (Ref. 36) and the spin diffusion length $\lambda_{sdl} = 1.4$ nm (Ref. 30), we estimate the real part of the spin mixing conductance to be $G_r = 6.5 \times 10^{14}$ Ω$^{-1}$m$^{-2}$.

In order to quantitatively determine the spin transmission across the interface, we measure the DL-SOT using the second harmonic Hall effect method.[26,31] We sweep an in-plane field applied along y to tilt the magnetization along this axis initially set to up or down orientation ($\mathbf{m_{up}}$, $\mathbf{m_{down}}$) and record the second harmonic resistance ($R^H_{2\omega}$). By neglecting the FL-SOT term whose contribution should scale with $R_{AHE}$ which is much smaller with respect to $R_{SMR}$, we can use the following simplified expression to quantify the effective field $h_{DL}$ corresponding to the DL-SOT (see Refs. 26 and 31 for more details)

$$R^H_{2\omega} = 2R_{SMR}\sin^2\theta\cos 2\varphi\frac{h_{DL}}{H_{ext}\sin\theta_H}. \quad (2)$$

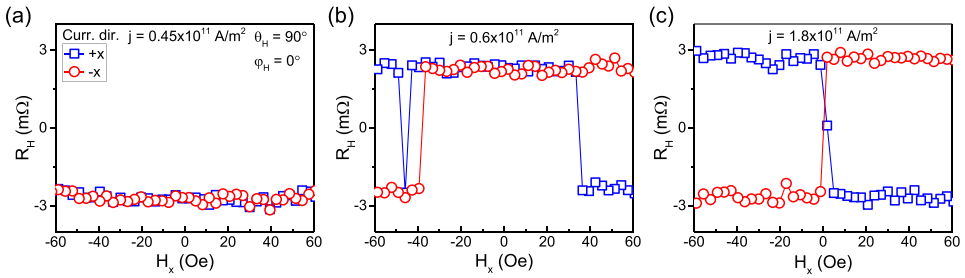


FIG. 2. The evolution of the switching behavior as a function of current amplitude. (a) No switching is observed for $j = 0.45 \times 10^{11}$ A/m$^2$. (b) Nearly 100% switching is obtained for field values $>35$ Oe when the current is increased to $j = 0.6 \times 10^{11}$ A/m$^2$. (c) Robust 100% switching is observed for $j = 1.8 \times 10^{11}$ A/m$^2$, down to $H_x = 2$ Oe.

In Fig. 1(d), we show $R^H_{2\omega}$ plotted versus $2R_{SMR}\sin^2\theta/H_y$ for $\mathbf{m_{up}}$ and $\mathbf{m_{down}}$ (note that $\cos 2\varphi = 1$ and $H_{ext}\sin\theta_H \equiv H_y$). Due to the DL-SOT symmetry, the effective field $h_{DL}$ changes sign between $\mathbf{m} \parallel \mathbf{z}$ and $\mathbf{m} \parallel -\mathbf{z}$ and hence the sign change of the slope. A linear fit yields $h_{DL} = 6.7 \pm 0.7$ Oe per $j \sim 0.8 \times 10^{11}$ A/m$^2$. We note that this value is $\sim$2 times larger than the previously reported value for TmIG(8 nm)/Pt(5 nm), indicating more efficient spin current through the interface, consistent with the larger SMR. By using the relation[10] $\theta_{SH} = \frac{2e}{\hbar}\frac{M_s t_F h_{DL}}{j}$, we estimate the spin Hall angle $\theta_{SH} \cong 0.03$.

We now focus on the quasi-DC switching experiments performed on the device described above using 10 ms-long current pulses. We followed a measurement procedure similar to Refs. 8 and 12, i.e., we stepped an in-plane field ($H_x$) applied along the x-axis and, at each field value, we applied positive and negative current pulses of equal amplitude measuring the Hall voltage $V_H$ after each pulse to monitor the magnetization state. Figures 2(a)–2(c) show representative measurements corresponding to three different currents. Within the field range $H_x < |\pm 60|$ Oe, we observe no switching event for $I = 0.9$ mA ($j = 0.45 \times 10^{11}$ A/m$^2$). However, upon injecting $I = 1.2$ mA ($j = 0.6 \times 10^{11}$ A/m$^2$), we observe current-induced switching at $|H_x| > 35$ Oe. By further increasing the current to $I = 3.6$ mA ($j = 1.8 \times 10^{11}$ A/m$^2$), we find that $\mathbf{m}$ switches for almost every $H_x$ value. At this current, within the resolution of the measurement, we determined the minimum $H_x$ required for switching to be $\sim$2 Oe, which is an extremely low value considering that $H_c = 100$ Oe and $H_K \approx 700$ Oe. We draw two important conclusions from these measurements. First, the threshold current for $|H_x| > 35$ Oe is $j = 0.6 \times 10^{11}$ A/m$^2$ which is $\sim$3 times lower than the previously reported value in TmIG/Pt measured under comparable conditions.[26] This result is consistent with the enhanced SMR and DL-SOT values found above and confirms the increase of the spin current transmission through the TmIG/Pt interface in our recent samples. Second, the minimum value of $H_x$ required for switching is exceptionally low, making this material highly suitable for efficient switching in heterostructures or chip carriers that produce moderate stray fields.

We now move on to the fast switching experiments using ns current pulses. We change the experimental setup to that described previously to facilitate efficient transmission of fast current pulses. Due to 100 kΩ resistances connected in series with the Hall voltage arms [see Fig. 1(a)], the signal-to-noise ratio in the $V_H$ measurements is significantly decreased with respect to quasi-dc measurements. For this reason, we use an alternative approach to probe the switching. We apply a constant $H_x$ and systematically change the pulse amplitude for a given constant pulse width. In order to enhance the signal-to-noise ratio, we repeat the positive-negative pulse sequence 25 times, measuring $V_H$ after each pulse and computing the average $\Delta V_H$.

Figures 3(a) and 3(b) show $V_H$ for 25 pulse counts for two different set pulse amplitudes $V_{set}$ and the same reset pulse $V_{reset} = -27$ V (pulse width set to $\tau_p = 20$ ns and $H_x = 177$ Oe). $V_{reset}$ was chosen to be large enough to switch $\mathbf{m}$ back to its initial up state after each set pulse. We notice that, despite the large fluctuations, a clear difference in $V_H$ after positive and negative pulses is evident for $V_{set} = 22$ V, which is absent when $V_{set} = 10$ V. By systematically varying $V_{set}$ between $+1$ V and $+33$ V, we find a threshold voltage $V_{set} = 19$ V, as depicted in Fig. 3(c). For this measurement, 1 V corresponds to $j = 0.52 \times 10^{11}$ A/m$^2$; therefore, the threshold current density is calculated as $j = 9.8 \times 10^{11}$ A/m$^2$, a value lower than the one obtained for Pt(3 nm)/Co(0.6 nm).[8] By normalizing $\Delta V_H$ by the change of $V_H$ obtained for full, field-induced reversal of the magnetization (not shown), we realize that the magnetization does not switch completely across the entire active region of the Hall cross, but rather only

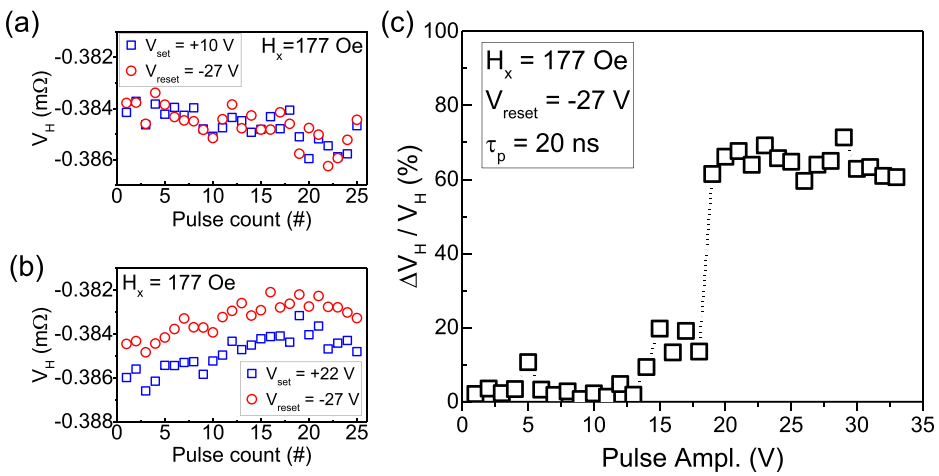


FIG. 3. (a) and (b) Measurement procedure to detect the switching with short current pulses. For a given field and set pulse amplitude, the Hall voltage ($V_H$) is measured after each pulse. The difference $\Delta V_H$ is averaged over 25 consecutive measurements to increase the signal-to-noise ratio. (c) $\Delta V_H$ normalized by $V_H$ to determine the % of switching and the threshold voltage (see text for more details).

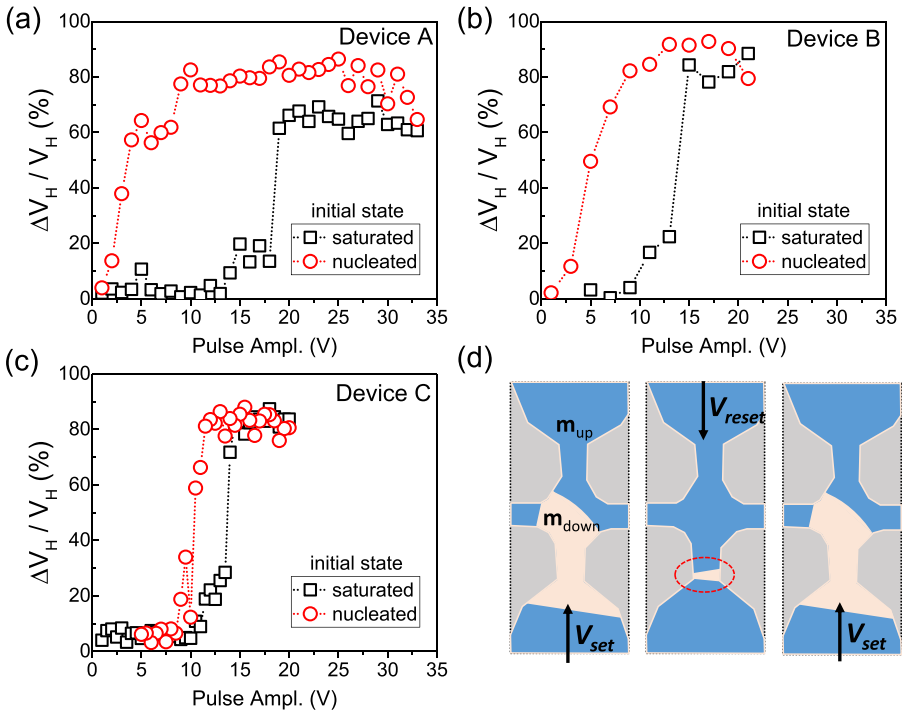


FIG. 4. (a)–(c) Determination of the switching threshold voltage for three different devices (A, B, and C). The black curves correspond to the forward sweep when started with a field-saturated state. The red curves correspond to the backward sweep where we believe that the magnetization is residually nucleated from the previous measurement; thereby, the threshold value is lower. (d) The assumed scenario is depicted. After the first switching event (left), $V_{reset}$ does not fully switch back **m** to fully up state and a small nucleated region remains (middle). Then, the switching occurs only by expanding and shrinking the domain outside the Hall cross region (right).

~60% of the Hall cross region is reversed. This behavior was consistent in several devices that we have studied and will be discussed below.

In order to obtain further insight into the partial switching of the device and verify the robustness of the threshold voltage, we have repeated the measurement by stepping the pulse amplitude in the reverse direction, i.e., going from larger to lower values. For the first device studied above, denoted "device A" hereafter, we found that the threshold value was reduced to 4 V, a factor of ~5 lower with respect to the forward sweep, as shown in Fig. 4(a). Further systematic measurements showed that when the magnetization is field-saturated by applying a large $H_z$ (approximately five times larger than $H_c$), the higher threshold value is observed, and after the first successful switching event, a lower current is sufficient to switch the magnetization. This two-threshold behavior was observed in three different devices as shown in Figs. 4(a)–4(c), measured in identical condition as in Device A, i.e., forward (black curves) and backward (red curves) stepping of the pulse amplitude, indicating that it is not due to sample specific defects.

A plausible explanation for the above observation is based on the different energy requirements for creating and translating domain walls. In micrometer-scale structures, SOT switching is usually mediated by domain nucleation and propagation.[36–38] Considering the Hall cross structure used here, it is likely that the first reverse domain is nucleated outside the cross where the arm width is lower and the current density is larger. Then, if the SOT is strong enough, the domain expands by the action of DL-SOT on the domain wall and the domain enters the central region of the cross and further expands towards the current injection lead, as depicted schematically in Fig. 4(d) (left panel). The partial switching is likely due to concerted result of tilted domain wall propagation under the action of SOT[38] and magnetic Hall arms obstructing the de-pinning of the slower side of the domain wall. We believe that in a well-defined (circular or square) magnetic dot, complete reversal can be achieved with similar current densities. By reversing the pulse polarity, i.e., by applying the reset pulse, the domain is expected to shrink and eventually disappear to set the magnetization back to the fully saturated state. However instead, our results suggest that after applying the reset pulse, a reverse domain remains outside the central cross region as shown in Fig. 4(d) (middle panel). Thus, after the first nucleation-propagation cycle, no nucleation is required and switching occurs solely by expanding-shrinking the domain back and forth by injecting a lower amplitude pulse [Fig. 4(d)–middle and right panels]. This might be the reason why a lower current is sufficient to switch the magnetization when the device is in the initially "nucleated" state. This scenario implies that the minimum energy or torque requirement to move the domain wall is much lower than to nucleate the first domain. In other words, the current-induced domain wall motion is efficient in this material and most of the energy to switch the magnetization is spent to nucleate the first reverse domain in the ns time regime.

Finally, we investigated the switching behavior with shorter current pulses ($\leq$5 ns). When we started from the field-saturated state, no switching was observed for pulses <15 ns (not shown), However, switching can be reliably obtained using pulses as short as 2 ns by pre-nucleating a domain outside the cross region, as shown in Fig. 5. We see that >50% switching can be achieved with pulses as short as 2 ns. Unfortunately, in the experimental setup, the maximum voltage that we could apply was limited to 35 V. Nevertheless, by assuming that the above nucleation arguments are valid, we can estimate the velocity of the domain wall motion. For 2 ns pulses at $V_{set}$=34 V (and $H_x$=171 Oe), we observe ~60% change in $\Delta V_H/V_H$ implying based on the geometry considerations a domain wall displacement of ~2 $\mu$m, assuming that the switching takes place by the expansion of a single domain. This means that at $j = 2.5 \times 10^{12}$ A/m$^2$, the domain wall moves at ~1000 m/s, i.e., ~400 m/s per $j = 1 \times 10^{12}$ A/m$^2$, a value exceeding the highest reported values for metallic ferromagnetic heterostructures.[18,39]

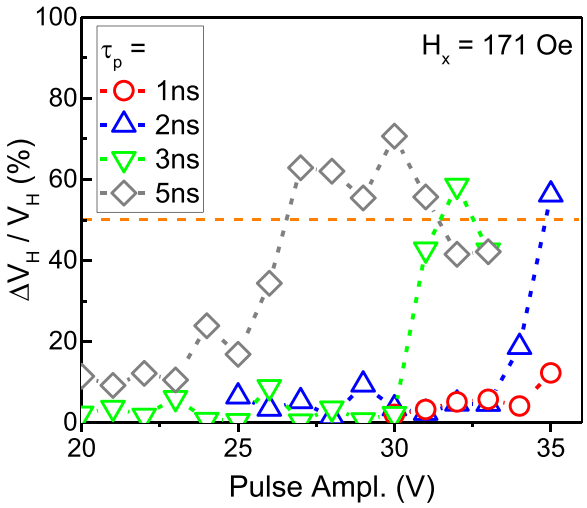


FIG. 5. Switching with current pulses shorter than 5 ns. We start with a state presumably containing a reverse domain and observe switching down to 2 ns pulses. For the proposed scenario (schematically depicted in Fig. 4), the domain wall must move several $\mu$m in order to achieve a 60% change of the Hall voltage $\Delta V_H/V_H$, which allows us to estimate a domain wall velocity of the order of 400 m/s per j= $1 \times 10^{12}$ A/m$^2$ in the non-thermally activated regime.

In conclusion, we have shown that an insulator with PMA can be switched by SOT with a remarkably low external field requirement of ~2 Oe. We further demonstrate that robust switching can be achieved with 20 ns pulses with current density $j < 1 \times 10^{12}$ A/m$^2$. We find that the threshold switching current strongly depends on the reversal history of the device. Our results suggest that this is due to the initial state of the magnetization which can be either saturated or possess reverse domains. Our proposed switching scenario implies that the domain wall can move very efficiently with current. Based on measurements with 2 ns pulses, we estimate the domain wall velocity in TmIG to be of the order of ~400 m/s per $j = 1 \times 10^{12}$ A/m$^2$, an exceptionally high value exceeding the most efficient domain wall velocities reported in metallic ferromagnets. These results are highly encouraging for the development of fast memory and logic devices based on magnetic insulators with perpendicular anisotropy.

This work was supported by C-SPIN, one of the six SRC STARnet Centers, sponsored by MARCO and DARPA, and the Swiss National Science Foundation. C.O.A. thanks Christoph Murer, Maxwell Mann, and Lucas Caretta for fruitful discussions, Aik Jun Tan for calibration of the Pt sputtering target, and Dr. Luqiao Liu for sharing ion miller equipment.

[1]C. Chappert, A. Fert, and F. N. Van Dau, Nat. Mater. **6**, 813 (2007).
[2]J.-E. Wegrowe, D. Kelly, Y. Jaccard, P. Guittienne, and J.-P. Ansermet, Eur. Lett. **45**(5), 626 (1999).
[3]M. Tsoi, A. G. M. Jansen, J. Bass, W. Chiang, M. Seck, V. Tsoi, and P. Wyder, Phys. Rev. Lett. **80**, 4281 (1998).
[4]J. Grollier, V. Cros, A. Hamzic, J.-M. George, H. Jaffres, A. Fert, G. Faini, J. Ben Youssef, and H. Legall, Appl. Phys. Lett. **78**, 3663 (2001).
[5]S. Mangin, D. Ravelosona, J. A. Katine, M. J. Carey, B. D. Terris, and E. E. Fullerton, Nat. Mater. **5**, 210 (2006).
[6]J. A. Katine and E. E. Fullerton, J. Magn. Magn. Mater. **320**, 1217 (2008).
[7]P. Gambardella and I. M. Miron, Philos. Trans. R. Soc. A **369**, 3175 (2011).
[8]I. M. Miron, K. Garello, G. Gaudin, P.-J. Zermatten, M. V. Costache, S. Auffret, S. Bandiera, B. Rodmacq, A. Schuhl, and P. Gambardella, Nature **476**, 189 (2011).
[9]K. Garello, I. M. Miron, C. O. Avci, F. Freimuth, Y. Mokrousov, S. Blügel, S. Auffret, O. Boulle, G. Gaudin, and P. Gambardella, Nat. Nanotechnol. **8**, 587 (2013).
[10]L. Liu, O. J. Lee, T. J. Gudmundsen, D. C. Ralph, and R. A. Buhrman, Phys. Rev. Lett. **109**, 96602 (2012).
[11]L. Liu, C.-F. Pai, Y. Li, H. W. Tseng, D. C. Ralph, and R. A. Buhrman, Science (80-) **336**, 555 (2012).
[12]C. O. Avci, K. Garello, I. M. Miron, G. Gaudin, S. Auffret, O. Boulle, and P. Gambardella, Appl. Phys. Lett. **100**, 212404 (2012).
[13]C.-F. Pai, L. Liu, Y. Li, H. W. Tseng, D. C. Ralph, and R. A. Buhrman, Appl. Phys. Lett. **101**, 122404 (2012).
[14]K. Garello, C. O. Avci, I. M. Miron, M. Baumgartner, A. Ghosh, S. Auffret, O. Boulle, G. Gaudin, and P. Gambardella, Appl. Phys. Lett. **105**, 212402 (2014).
[15]G. Yu, P. Upadhyaya, Y. Fan, J. G. Alzate, W. Jiang, K. L. Wong, S. Takei, S. A. Bender, L. Chang, Y. Jiang, M. Lang, J. Tang, Y. Wang, Y. Tserkovnyak, P. K. Amiri, and K. L. Wang, Nat. Nanotechnol. **9**, 548 (2014).
[16]X. Qiu, K. Narayanapillai, Y. Wu, P. Deorani, D.-H. Yang, W.-S. Noh, J.-H. Park, K.-J. Lee, H.-W. Lee, and H. Yang, Nat. Nanotechnol. **10**, 333–338 (2015).
[17]S. Fukami, T. Anekawa, C. Zhang, and H. Ohno, Nat. Nanotechnol. **11**, 621 (2016).
[18]I. M. Miron, T. Moore, H. Szambolics, L. D. Buda-Prejbeanu, S. Auffret, B. Rodmacq, S. Pizzini, J. Vogel, M. Bonfim, A. Schuhl *et al.*, Nat. Mater. **10**, 419 (2011).
[19]S. Emori, U. Bauer, S.-M. Ahn, E. Martinez, and G. S. D. Beach, Nat. Mater. **12**, 611 (2013).
[20]K. Ryu, L. Thomas, S. Yang, and S. Parkin, Nat. Nanotechnol. **8**, 527 (2013).
[21]P. P. J. Haazen, E. Murè, J. H. Franken, R. Lavrijsen, H. J. M. Swagten, and B. Koopmans, Nat. Mater. **12**, 299 (2013).
[22]J. Torrejon, J. Kim, J. Sinha, S. Mitani, M. Hayashi, M. Yamanouchi, and H. Ohno, Nat. Commun. **5**, 4655 (2014).
[23]B. H. A. A. Serga and A. V. Chumak, J. Phys. D: Appl. Phys. **43**, 264002 (2010).
[24]A. D. Karenowska, A. V. Chumak, A. A. Serga, and B. Hillebrands, Handb. Spintron. **11**, 1505 (2015).
[25]A. Quindeau, C. O. Avci, W. Liu, C. Sun, M. Mann, A. S. Tang, M. C. Onbasli, D. Bono, P. M. Voyles, Y. Xu, J. Robinson, G. S. D. Beach, and C. A. Ross, Adv. Electron. Mater. **3**, 1600376 (2016).
[26]C. O. Avci, A. Quindeau, C.-F. Pai, M. Mann, L. Caretta, A. S. Tang, M. C. Onbasli, C. A. Ross, and G. S. D. Beach, Nat. Mater. **16**, 309 (2017).
[27]C. Tang, P. Sellappan, Y. Liu, Y. Xu, J. E. Garay, and J. Shi, Phys. Rev. B **94**, 140403(R) (2016).
[28]A. Ghosh, K. Garello, C. O. Avci, M. Gabureac, and P. Gambardella, Phys. Rev. Appl. **7**, 014004 (2017).
[29]H. Nakayama, M. Althammer, Y. T. Chen, K. Uchida, Y. Kajiwara, D. Kikuchi, T. Ohtani, S. Geprägs, M. Opel, S. Takahashi, R. Gross, G. E. W. Bauer, S. T. B. Goennenwein, and E. Saitoh, Phys. Rev. Lett. **110**, 206601 (2013).
[30]Y.-T. Chen, S. Takahashi, H. Nakayama, M. Althammer, S. Goennenwein, E. Saitoh, and G. Bauer, Phys. Rev. B **87**, 144411 (2013).
[31]C. O. Avci, A. Quindeau, M. Mann, C. Pai, C. A. Ross, and G. S. D. Beach, Phys. Rev. B **95**, 115428 (2017).
[32]J. Li, G. Yu, C. Tang, Y. Liu, Z. Shi, Y. Liu, A. Navabi, M. Aldosary, Q. Shao, K. L. Wang, R. Lake, and J. Shi, Phys. Rev. B **95**, 241305(R) (2017).
[33]M. Althammer, S. Meyer, H. Nakayama, M. Schreier, S. Altmannshofer, M. Weiler, H. Huebl, S. Gepr, M. Opel, R. Gross, D. Meier, C. Klewe, T. Kuschel, J. Schmalhorst, L. Shen, A. Gupta, Y. Chen, E. Saitoh, and S. T. B. Goennenwein, Phys. Rev. B **87**, 224401 (2013).
[34]N. Vlietstra, J. Shan, V. Castel, B. J. Van Wees, and J. Ben Youssef, Phys. Rev. B **87**, 184421 (2013).
[35]M. Isasa, A. Bedoya-pinto, S. Vélez, F. Golmar, F. Sánchez, L. E. Hueso, and F. Golmar, Appl. Phys. Lett. **105**, 142402 (2014).
[36]O. J. Lee, L. Q. Liu, C. F. Pai, Y. Li, H. W. Tseng, P. G. Gowtham, J. P. Park, D. C. Ralph, and R. A. Buhrman, Phys. Rev. B **89**, 24418 (2014).
[37]J.-C. Rojas-Sanchez, P. Laczkowski, J. Sampaio, S. Collin, K. Bouzehouane, N. Reyren, H. Jaffres, A. Mougin, and J.-M. George, Appl. Phys. Lett. **108**, 82406 (2016).
[38]M. Baumgartner, K. Garello, J. Mendil, C. O. Avci, E. Grimaldi, C. Murer, J. Feng, M. Gabureac, C. Stamm, Y. Acremann, S. Finizio, S. Wintz, J. Raabe, and P. Gambardella, Nat. Nanotechnol. (in press).
[39]S. Yang, K. Ryu, and S. Parkin, Nat. Nanotechnol. **10**, 221 (2015).